British Journal of Applied Science & Technology
4(20): 2878-2890, 2014

SCIENCEDOMAIN *international*
www.sciencedomain.org

Design and Calibration of a Low Speed Wind Tunnel

R. Ramkissoon[1] and K. Manohar[1*]

[1]Mechanical and Manufacturing Engineering Department, The University of the West Indies, St. Augustine, Trinidad and Tobago, West Indies.

Authors' contributions

This work was carried out in collaboration between the two authors. Author RR designed the study, performed the experiments and analysis and wrote the first draft of the manuscript. Author KM managed the analyses of the study, reviewed and edited the manuscript for submission, managed all correspondence and addressed all concerns of the reviewers. Both authors read and approved the final manuscript.

Original Research Article

Received 14th March 2014
Accepted 7th May 2014
Published 22nd May 2014

ABSTRACT

A low speed, open circuit, laboratory wind tunnel was designed and built to facilitate the testing of airfoils designed for use with straight bladed vertical axis wind turbines. The wind tunnel built was the open-circuit type and was chosen due to the ease of fabrication and low construction costs associated with the build. Wind speed through the tunnel was controlled by a variable speed WEG 3.00 hp motor drive unit with a WEG CFW 08 vector inverter plus motor speed control unit. Calibration tests were performed using a hot-wire anemometer to determine the wind velocity as a function of differential pressure measured using a pressure transducer. The characteristic curve of wind velocity vs inches of water was plotted. The velocity profile for this wind tunnel indicated a turbulent flow regime and there was a good second order polynomial relationship between the measured velocity and differential pressure drop.

Keywords: Wind tunnel; diffuser; contraction cone; velocity profile.

**Corresponding author: E-mail: krishpersad.manohar@sta.uwi.edu;*

NOMENCLATURE

A	Area
β	Open area ratio
B	Constant
d	Wire diameter
d	Cylinder diameter
D_H	Hydraulic Diameter
D_{eff}	Effective Diameter
ε	Roughness factor
f	Friction factor
g	Gravity
δ^*	Boundary layer
k	Constant
K	Screen pressure drop coefficient
L	Length of screen
ρ	Density
P	Pressure
P	Wetted Perimeter
Re	Reynolds Number
τ_0	Shear stress
u	Streamwise fluctuating velocity
u_*	Friction velocity
v	Vertical fluctuating velocity
V	Velocity
y	Distance from wall

1. INTRODUCTION

The wind tunnel is one of the most common experimental testing facilities for the testing of fluid flow [1,2]. There are many types of wind-tunnels and they can be classified by the flow speed which can divide them into four groups.

- Subsonic or low-speed wind-tunnels.
- Transonic wind-tunnels.
- Supersonic wind-tunnels.
- Hypersonic wind-tunnels.

Wind-tunnel design is a complex field involving fluid mechanics and engineering aspects [3, 4]. The main advantage of the open circuit wind tunnel is in the savings of space and cost. Also, the effect of temperture changes is small and the performance of a fan fitted at the upstream end is not affected by disturbed flow from the working section [5].

The quality of results from experimental measurements obtained around a model in a wind tunnel is dependent on the quality of the free-stream flow. Assuring a high quality free-stream flow is of particular interest for investigations of external flows involving separated shear layers, e.g., separation on a wing, or wake of a bluff body [5]. The quality of the flow in a wind tunnel is mainly characterized by two features, namely, flow uniformity and turbulence intensity. Wind-tunnels represent a useful tool for investigating various flow phenomena. An

advantage of using wind-tunnels is that experiments can be performed under controlled flow circumstances compared to experiments in the open environment.

The design of wind tunnel contractions has been based on a pair of cubic polynomials, and the parameter used to optimize the design for a fixed length and contraction ratio, has been the location of the joining point [6,7].

2. DESCRIPTION OF WIND TUNNEL

In this study the proposed design was an open-circuit suction wind tunnel in which the airflow was completely contained within the wind tunnel laboratory. The air leaving the wind tunnel via the fan flowed through the laboratory room and back through a filter and screen into the wind tunnel. The wind tunnel was the conventional non-return type with one closed working section and was constructed using 9.490 mm thick plywood. The dimensions of the wind tunnel was 3.912 m in overall length, 1.626 m wide and 1.626 m high at the mouth as shown in the schematic, Fig. 1.

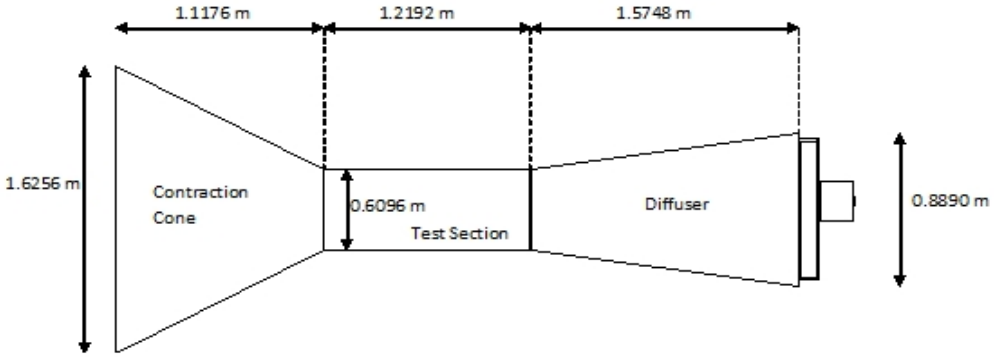

Fig. 1. Schematic diagram of the wind tunnel

Wind speed through the tunnel was controlled by a variable speed WEG 3.00 hp motor drive unit with a WEG CFW 08 vector inverter plus motor speed control unit. Wind speeds of 3 m/s ~ 16 m/s were obtained in the wind tunnel over the test section. The hot-wire anemometer position was 2.184 m upwind from the wind-tunnel exit. This area had a stable, uniform flow condition. At this point the working section was 1.219 m wide and 0.6096 m high.

The purpose of building this wind tunnel was to facilitate testing of airfoils at low speeds at the University of the West Indies, St Augustine campus. The primary aim was to accommodate experiments that require using airfoils prototypes and placement of endplates in the test section geometry. The main design criteria were:

1. Open circuit wind-tunnel.
2. Good flow quality.
3. Contraction ratio, CR, of 6-9.
4. Test section aspect ratio of 2 and the maximum test section length possible in the available space.
5. Flow speed in the test section between 3 m/s to 15 m/s.
6. Low noise level.
7. Low cost.

Along with wind tunnel geometry, such as contraction ratio, these flow features were controlled by turbulence manipulating devices, located upstream of the test section. The two most effective turbulence manipulators are honeycomb and mesh screens, each of which serves a specific purpose [5]. The reduction in turbulence intensity for flow through a screen is a function of the screen's pressure drop coefficient (K), which can be calculated using the following formula (equation 1) developed by Wieghardt [8], as recommended by Bradshaw & Mehta [9].

$$K = 6.5\left(\frac{1-\beta}{\beta}\right)\left(\frac{Ud}{\beta v}\right)^{\frac{-1}{3}} \quad (1)$$

In this equation, β is the open area ratio, u is steamwise fluctuating velocity, v is vertical fluctuating velocity and d is the cylinder diameter.

Turbulence reduction increases with the pressure drop coefficient. From equation 1, K increases with decreasing β; however, Bradshaw & Mehta [9] stated that for β < 0.58 flow non-uniformities starts to develop. Therefore, optimal turbulence reduction is achieved when multiple screens of relatively high open area ratio (β > 0.58) are utilized in series. In this case β is given by equation 2.

$$\beta = \left(1 - \frac{d}{L}\right)^2 \quad (2)$$

where d is the wire diameter and L is the length of the screen

3. DESIGN AND CONSTRUCTION

3.1 Test Section Assembly

The test section was built from 6.35 mm thick Plexiglas and attached together with silicone and L-Brackets. The dimensions of the test section assembly were 60.96 cm x 60.96 cm and 121.92 cm in length. Fig. 2 shows a picture of the completed test section.

Fig. 2. Wind Tunnel Test Section

3.2 The Diffuser Assembly

This assembly housed the fan and electrical wiring for the fan and fan controller. The diffuser assembly was fabricated using 9.525 mm plywood. The first part of the Diffuser Assembly's construction was the Drive Section. This composed of a 77.47 cm diameter fan and the 90.17 cm x 90.17 cm aluminum fan housing (Fig. 3).

Fig. 3. The fan assembly

The area of the Drive Section (the large end of the Diffuser) was 0.79 m^2 which is 2.127 times the area of the end of the Test Section (also the area of the small end of the Diffuser). According to Cockrell and Markland [10] best results are achieved for a ratio is 2:1. The dimension of the diffuser body was 0.790 m^2 tapered to 0.403 m^2 with a length of 1.575 m. The plywood was then attached to one another with nails and silicone was then used to seal the joining. The completed Diffuser assembly is shown in Fig. 4.

Fig. 4. The diffuser assembly

3.3 Contraction Cone Assembly

This assembly was at the forward end of the tunnel into which the air flowed as it was drawn in by the fan at the back. This assembly consisted of the Contraction Cone and the Settling Chamber. The body of the contraction cone was also made with 9.525 mm plywood. Nails were used to connect the plywood together and sealed with silicone.

3.3.1 Settling chamber

This component was made with two honeycomb mesh and one screen in the large end of the Contraction Cone, to reduce turbulence to a minimum and improves airflow quality. The screen reduced streamwise velocity fluctuations. To find the screen's pressure drop coefficient (K) from equation 1, the open area ratio β from equation 2 was calculated using the wire diameter, d as 0.2 mm and l (length of screen) as 0.9 mm.

$$\beta = (1 - 0.20/0.90)^2 = 0.605$$

This value is greater than 0.58 (for $\beta < 0.58$ flow non-uniformities start to develop [9].

The honeycomb with its cell aligned in the flow direction will reduce minor fluctuating variations in transverse velocity with little effect on steamwise velocity because the pressure drop through a honeycomb is small. The honeycomb used was 90 mm long and the hexagonally shaped cells had a diameter of 15 mm i.e. the length to diameter ratio of the cells was about 6. For optimum benefit the cell length should be about 6-8 times its diameter [9].

The primary reason for using the honeycomb is that, with a sufficient length of about 6-8 cell diameters [4], it forms a very effective flow straightening device. The relatively low pressure drop of a honeycomb made it rather ineffective in reducing non-uniformities or fluctuations in the stream wise component but it is very effective in reducing cross-stream components [11].

3.3.2 Contraction cone body

The contraction section was located between the settling chamber and the test sections and served to both increase mean velocities at the test section inlet and moderate inconsistencies in the uniformity of the flow. Large contraction ratios and short contraction lengths are generally more desirable as they reduce the power loss across the screens and the thickness of boundary layers. Small tunnels typically have contraction ratios between 6 and 9 [5]. The area of the entry to the contraction cone was 2.643 square meters. The exit from the contraction cone to the test section was 0.403 square meters. The contraction ratio was therefore 6.55. A description of the main components of the wind tunnel and the associated cost are shown on Table 1.

Table 1. Description of the wind-tunnel parts with associated cost.

Part	Description	Cost (US Dollars)
Test section	60.96 cm x 60.96 cm and 121.92 cm in length	125.00
Diffuser	0.790 m^2 tapered to 0.403 m^2 with a length of 1.575 m	20.00
Fan	(D = 77.47 cm; P = 2.2 kW)	500.00
Honeycomb	length to diameter ratio of the cells is 6	40.00
Screens	open area ratio (β) of 0.58	70.00
Contraction	Contraction ratio of 6.55	20.00

4. CALIBRATION OF THE WIND TUNNEL

Experimental measurements were conducted to calibrate the laboratory built wind tunnel. Wind speed through the tunnel was controlled by a variable speed WEG 3.00 hp motor drive unit with a WEG CFW 08 vector inverter plus motor speed control unit. Calibration measurements included the boundary layer velocity profile and the wind velocity verses inches of water expressed in terms of milliamps, in the working section, in terms of the differential pressure values in the contraction cone. Calibration tests were performed using a hot-wire anemometer to determine the wind velocity as a function of differential pressure measured using a pressure transducer

4.1 Anemometer Selection

The hotwire anemometer used was the Amprobe TMA20HW. The Amprobe TMA20HW Hot Wire anemometer technology eliminates the use of bearings and rotating parts. The meter is durable and provides good and stable accuracy of the measurements. This is a highly accurate anemometer with 0.1% basic accuracy for precise measurements with an air flow measurements range of 0.3 m/s to 30.0 m/s. The electrical specifications of the Amprobe TMA20HW anemometer are listed below in Table 2.

Table 2. Electrical specifications of the Amprobe anemometer

Feature	Range	Accuracy
Air Flow	0.1 to 30 m/s	±3% of reading
	0.2 to 110 km/hr	±1% FS
	10 to 6000 ft/min	
	0.1 to 59 knots	
	0.12 to 68 MPH	
Air flow Volume	0.0 to 9999 CFM	±1% FS
Temperature	-20^{o}C to 60^{o}C	±0.5^{o}C
	-4 F to 140 F	±0.9 F
Humidity	0.0 to 100 %	±3% RH

4.2 Differential Pressure Sensor Selection

In order to determine the right pressure sensor for the wind tunnel, preliminary tests measured the pressure range for its location. This was done using the wind speed at different locations in the wind tunnel. Experiments performed in the Open Wind Tunnel with a hot wire anemometer showed that the velocity ranged between 3 m/s to 16 m/s. This was related to the dynamic pressure by using Bernoulli's Equation:

$$P_o = P_\infty + \frac{\rho V^2}{2} \quad (3)$$

This equation ignored the effects of compressibility, which was a good assumption for low speed flows. To find how this relates to the tunnel measuring system, or inches of a water column, equation 4 was used.

$$P = \rho g h \quad (4)$$

The unit used to measure the pressure difference was inches of a water column. To find out the largest pressures a combination of equations 3 and 4 was used. The dynamic pressure in Bernoulli's equation can be set equal to the dynamic pressure in equation 4.

$$\frac{\rho V^2}{2} = \rho g h \tag{5}$$

To determine the height of the water column equation 6 can be used.

$$h = \frac{\rho_{air} V^2}{2\rho_{water} g} \tag{6}$$

Substituting ρ_{air} – 1.145 kg/m^3, V – 16 m/s, ρ_{water} – 995 kg/m^3, g – 9.806 m/s^2.

This gave a value of 0.015 m, which is 0.592 inches.

Using this data, the Setra Model M264 Differential Pressure Transmitter was selected for this wind tunnel. This low-air pressure transmitter capable of sensing differential pressure in both negative and positive ranges. The Model M264 incorporates a tensioned stainless steel diaphragm to form a variable capacitor that will produce variation in the output signal (4mA to 20mA). It's specifications are listed below in Table 3.

Table 3. Specifications of the Setra Model M264 Differential Pressure [12]

Specifications		**Specifications**	
Supply Voltage	**9 to 33 VDC**	**Operating Temp**	**-18ºC to 79ºC**
Signal Output	4 – 20 mA (two wire); Voltage 0 – 5 VDC (three wire)	Additional specification Range	Unit is factory calibrated at 0g Zero offset (%FC/g)
Accuracy	±1% FS, RSS (at constant temp) 0.1% FS Hysteresis 0.2%FS	Up to 0.5" WC Up to 1.0" WC Up to 2.5" WC Up to 5.0" WC	0.06 0.05 0.22 0.14
Maximum Output Impedance mA	800Ω @24 VDC	Process Connection	3/16" OD barbed brass
Minimum Output Impedance VDC	≥ 5000 Ω	Enclosure rating	Glass-filled polyester
Repeatability	0.05% FS	Temp range Approvals	0to150 F(-18to65ºC) CE
Thermal Effect	Compensated temperature range 0 to 150 F (-18 to 65ºC) Zero/Span shift o.033 F (0.018ºC)	Overpressure Hysteresis Dimensions	Up to 10 psig (68.95 kPa) range dependant ±0.1% FC 14x7.62x4.85 cm
Weight	0.55 lb (0.25 kg)	Warranty	3 years

5. RESULTS

The free-stream speed within the test section was set by measuring the pressure drop across the 6.55:1 contraction. The pressure drop was calibrated against the hot wire anemometer positioned in the mid-span of the test section. The contraction pressure drop was monitored by a Setra Model M264 Differential Pressure Transmitter, while the hot wire anemometer used was an Amprobe TMA20HW. The free-stream speed was obtained from a calibration curve of the wind velocity versus contraction pressure drop in inches of water expressed in terms of milliamperes. Figs. 5 and 6 shows a graphical representation of the results obtained.

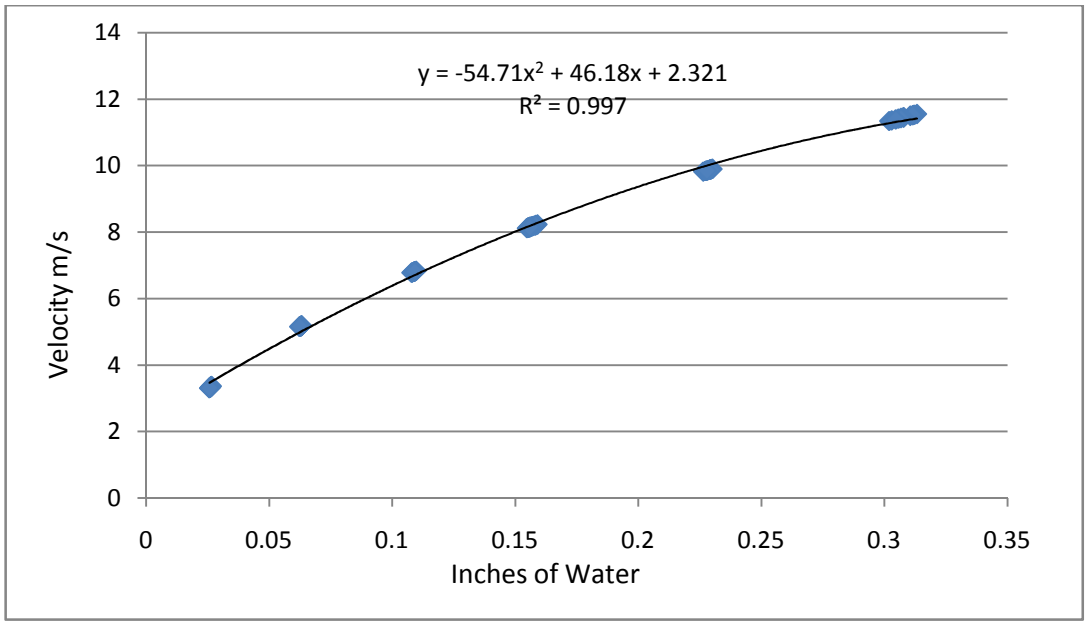

Fig. 5. Wind Velocity vs inches of water

5.1 Velocity Profile

Data for the velocity profiles was obtained with the fan kept at a constant setting and measurements were taken at incremental distances from the wall. The stem of the hot wire anemometer was marked off in ten millimeter increments. These results are displayed in Figs. 7 and 8.

The Reynolds number was calculated from equation 7 and varied from 118,482 to 413,434 this indicated that the flow was turbulent (Re > 4000).

$$Re_x = \frac{\rho U D_H}{u} \tag{7}$$

For turbulent flow in a square duct we have to use the hydraulic diameter, D_H.

$$D_H = \frac{4A}{P} \tag{8}$$

where A is the area and P is the wetted perimeter.

For turbulent flow in a square duct the shear is nearly constant along the sides, dropping off sharply to zero in the corners. This is because of the phenomenon of turbulent secondary flows in which there are non-zero mean velocity, v and w in the plane of the cross-section. The Hydraulic diameter for this test section is 0.6096 m.

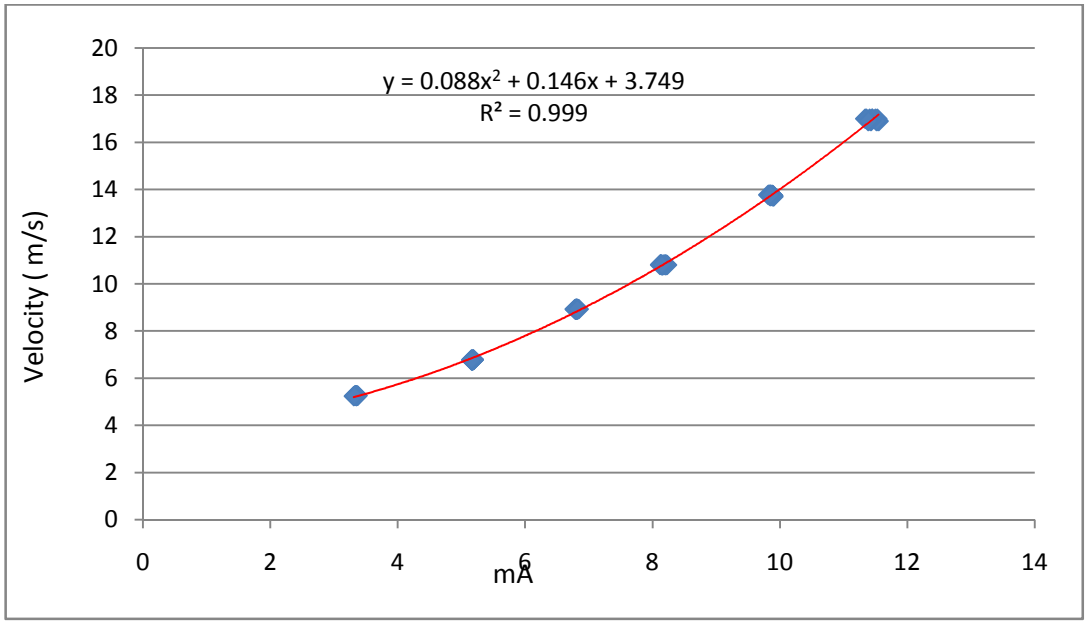

Fig. 6. Wind Velocity vs milliamps

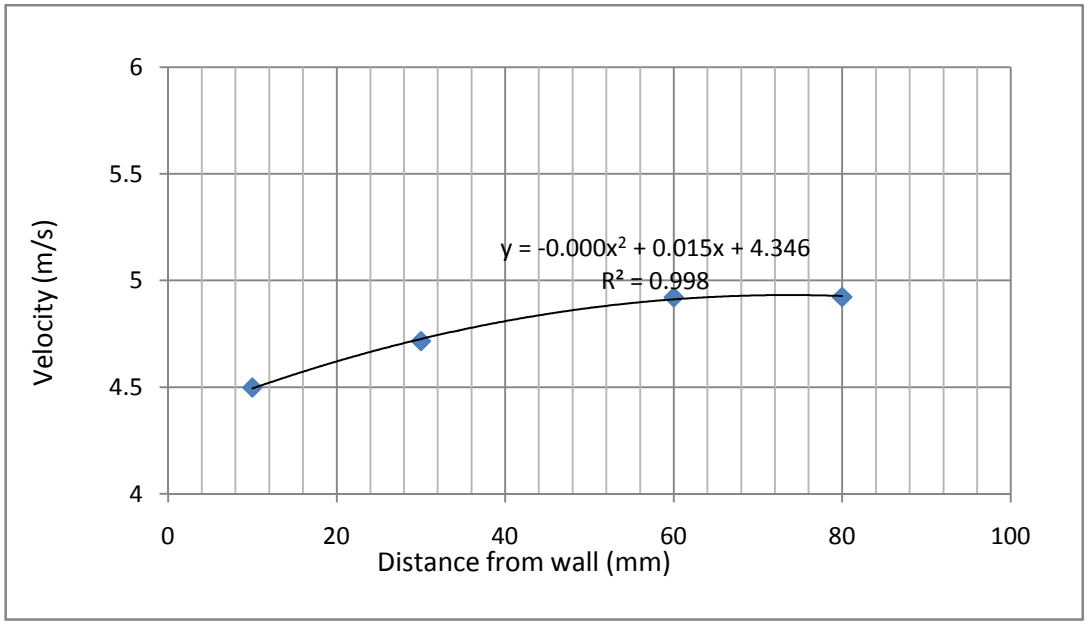

Fig. 7. Wind velocity vs. wall distance

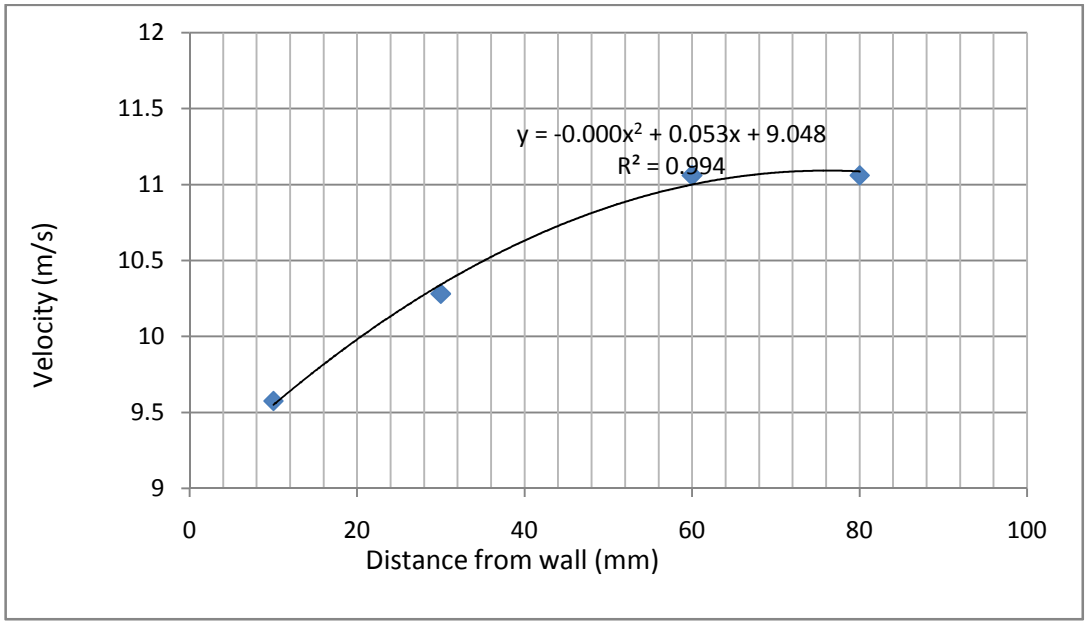

Fig. 8. Wind velocity vs. wall distance

From documented data [14], b/a = 1. The effective diameter was calculated from equation 9.

$$\boldsymbol{D_{eff}} = \frac{\mathbf{64}}{\mathbf{56.91}}\boldsymbol{D_H} \tag{9}$$

The effective diameter was 0.6855 m.

Equation 10 is the friction velocity.

$$\boldsymbol{u^*} = \left(\frac{\tau_w}{\rho}\right)^{1/2} \tag{10}$$

The velocity profile for turbulent flow was

$$\boldsymbol{v} = \boldsymbol{u^*}\left(\frac{\mathbf{1}}{\boldsymbol{k}}\,\boldsymbol{ln}\frac{\boldsymbol{hu^*}}{\boldsymbol{v}} + \boldsymbol{B} - \frac{\mathbf{1}}{\boldsymbol{k}}\right) \tag{11}$$

where k is 0.41, B is 5.0 and h is the distance from the centre line to the wall of the test section.

The roughness factor for Plexiglas [13,14], ε – 0.0015 mm.

Now ε/D_H = 0.00000246. Using the Moody chart [15] the friction factors (f) were read off. Using equation 12.

$$\frac{\boldsymbol{v}}{\boldsymbol{u^*}} = \left(\frac{\boldsymbol{\delta^*}}{\boldsymbol{f}}\right)^{1/2} \tag{12}$$

where the boundary layer separation is

$$\boldsymbol{\delta^*} = \frac{\mathbf{1.721}\boldsymbol{x}}{\boldsymbol{Re_x^{1/2}}} \tag{13}$$

6. DISCUSSION

The first test was to produce the velocity profile for this wind tunnel. From Figs. 7 and 8 the results indicate a turbulent flow regime. A lease squares second-degree polynomial curve displayed an almost exact fit to the data with R^2 values of 0.998 and 0.995. The plot of mean velocity vs. distance from the tunnel wall was compared with the profile for turbulent flow in a square duct (Fig. 9).

The experimental data matched closely to the turbulent flow curve indicating that the wind speed was under 12 m/sec and the flow was turbulent. This can be possible if the fan was inducing sufficient unsteadiness in the flow.

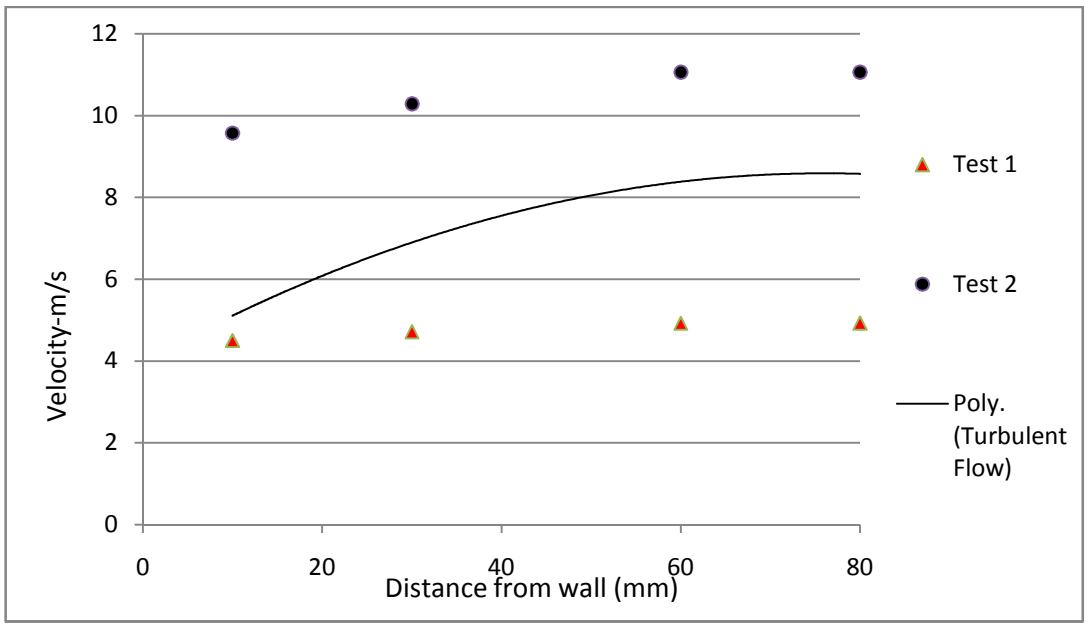

Fig. 9. Turbulent velocity profiles

The second test was to establish a relationship between the measured wind velocities to the differential pressure drop in inches of water expressed in milliamps. Fig. 6 shows a second order polynomial relationship between the measured velocity and milliamps with a lease squares data fit showing an R value of 0.9995. Again, this is almost an exact fit, indicating that the data fits very well to the line. Also, from the graph (Fig. 6), it appears that electronic and mechanical noise was not a very big problem and the equation of the regression line, $y = 0.0881x^2 + 0.146x + 3.7497$, can be used to calculate the wind velocity when the wind tunnel is being used for testing airfoils via the differential pressure reading in the contraction cone. It indicates that the pressure sensor calibration was a second order polynomial fit.

7. CONCLUSION

1. A turbulent flow regime was noticed in the vertical boundary layer of the wind tunnel.
2. There is a second order polynomial relationship between the wind velocity and the differential pressure drop across the contraction cone section. The R squared value was 0.9995.

3. Electronic and mechanical noise was not a affecting the differential pressure transducer output.
4. The equation derived from the plot of wind velocity vs. milliamps (inches of water) can be used to calculate the wind velocity when the wind tunnel is to be used for testing airfoils. (Wind speed through the tunnel was controlled by a variable speed WEG 3.00 hp motor drive unit with a WEG CFW 08 vector inverter plus motor speed control unit).
5. The total cost was $ 775.00 US dollars.

COMPETING INTERESTS

Authors have declared that no competing interests exist.

REFERENCES

1. Pope A. Low-Speed Wind Tunnel Testing. John Wiley and Sons, New York; 1966.
2. Tavoularis, Stavros. Measurement in Fluid Mechanics, Cambridge University Press; 2005.
3. Rae WH, Pope A. Low-speed wind tunnel testing. 2nd edition. John Wiley & sons; 1984.
4. Bradshaw P, Pankhurst RC. The design of low-speed wind tunnels. Progress in Aeronautical Sciences. 1964;6:1-69.
5. Mehta RD, Bradshaw P. Design Rules for Small Low Speed Wind Tunnels. Aeronautical Journal. 1979;443-449.
6. Morel T. Comprehensive Design of Axisymmetric Wind Tunnel Contractions. ASME Journal of Fluids Engineering. 1975;225-233.
7. Ramaseshan S, Ramaswamy MA. A Rational Method to Choose Optimum Design for Two-Dimensional Contractions. ASME Journal of Fluids Engineering. 2002;124:544-546.
8. Wieghardt. On the Resistance of Screens, Aero. Quarterly, Royal Aero Society. 1953;4.
9. Bradshaw P, Mehta R. Wind Tunnel Design; 2003.
   Available: http://www.htglstanford.edu/ bradshaw/tunnel/wadiffuser.html
10. Cockrell DJ, Markland E. Diffuser behavior, a review of past experimental work, relevant today. Aircr Engng.1974;46:16.
11. Scheiman J, Brooks JD. Comparison of experimental and theoretical turbulence reduction from screens, honeycomb and honeycomb-screen combinations. JAS. 1981;18:638-643.
12. Available: www.setra.com/.../Pressure/Differential-Pressure/Air.../264-Data-Sheet.as
13. Moody LF. Friction factors for Pipe Flow. ASME Trans. 1944;66:671-684.
14. White MF. Fluid Mechanics. McGraw-Hill Inc, New York. 1994;333.

Peer-review history:
The peer review history for this paper can be accessed here:
http://www.sciencedomain.org/review-history.php?iid=537&id=5&aid=4654